

## The magnetic properties of $\text{MMCo}_5$ (MM=Mischmetal) nanoflakes prepared by multistep (three steps) surfactant-assisted ball milling

X. Zhao, W. L. Zuo, M. Zhang, D. Liu, J. F. Xiong, R. X. Shang, J. Zhang, T. Y. Zhao, J. R. Sun, and B. G. Shen

Citation: *AIP Advances* **7**, 056203 (2017);

View online: <https://doi.org/10.1063/1.4973395>

View Table of Contents: <http://aip.scitation.org/toc/adv/7/5>

Published by the [American Institute of Physics](#)

---

### Articles you may be interested in

[Magnetic properties of Sm-Fe-N bulk magnets produced from Cu-plated Sm-Fe-N powder](#)

*AIP Advances* **7**, 056204 (2016); 10.1063/1.4973396

[Structure and properties of sintered MM-Fe-B magnets](#)

*AIP Advances* **7**, 056215 (2017); 10.1063/1.4973603

[Magnetic properties of \(misch metal, Nd\)-Fe-B melt-spun magnets](#)

*AIP Advances* **7**, 056207 (2017); 10.1063/1.4973846

[Magnetic properties of  \$\text{Nd}\(\text{Fe}\_{1-x}\text{Co}\_x\)\_{10.5}\text{M}\_{1.5}\$  \(M=Mo and V\) and their nitrides](#)

*AIP Advances* **7**, 056202 (2016); 10.1063/1.4973207

[Micromagnetic simulation of the influence of grain boundary on cerium substituted Nd-Fe-B magnets](#)

*AIP Advances* **7**, 056201 (2016); 10.1063/1.4972803

[Coercivity of Nd-Fe-B hot-deformed magnets produced by the spark plasma sintering method](#)

*AIP Advances* **7**, 056205 (2016); 10.1063/1.4973438

---

# HAVE YOU HEARD?

Employers hiring scientists and engineers trust

**PHYSICS TODAY | JOBS**

[www.physicstoday.org/jobs](http://www.physicstoday.org/jobs)



## The magnetic properties of $\text{MMCo}_5$ (MM=Mischmetal) nanoflakes prepared by multistep (three steps) surfactant-assisted ball milling

X. Zhao,<sup>1,2</sup> W. L. Zuo,<sup>1</sup> M. Zhang,<sup>1</sup> D. Liu,<sup>1,2</sup> J. F. Xiong,<sup>1,2</sup> R. X. Shang,<sup>1,2</sup> J. Zhang,<sup>1,2</sup> T. Y. Zhao,<sup>1,2</sup> J. R. Sun,<sup>1,2</sup> and B. G. Shen<sup>1,2,a</sup>

<sup>1</sup>State Key Laboratory of Magnetism, Institute of Physics, Chinese Academy of Sciences, Beijing 100190, People's Republic of China

<sup>2</sup>University of Chinese Academy of Sciences, Beijing 100049, People's Republic of China

(Presented 1 November 2016; received 23 September 2016; accepted 17 October 2016; published online 27 December 2016)

The hard magnetic  $\text{MMCo}_5$  nanoflakes with high coercivity and narrow size distribution have been successfully obtained by three steps surfactant-assisted ball milling (SABM). The magnetic properties, phase structure and morphology of these  $\text{MMCo}_5$  nanoflakes were studied in this work. The coercivity and the remanence ratio of  $\text{MMCo}_5$  nanoflakes reached to 5.89 kOe and 0.75, respectively. The X-ray powder diffraction (XRD) patterns indicated that the  $\text{MMCo}_5$  nanoflakes were  $\text{CaCu}_5$ -type hexagonal crystal structure. The average thickness, in-plane size and aspect ratio reached to 20 nm, 0.9  $\mu\text{m}$  and 60, respectively. The low cost and great properties of  $\text{MMCo}_5$  nanoflakes with a centralized thickness distribution could be the building blocks for the future high-performance nanocomposite permanent magnets with an enhanced energy product. © 2016 Author(s). All article content, except where otherwise noted, is licensed under a Creative Commons Attribution (CC BY) license (<http://creativecommons.org/licenses/by/4.0/>). [<http://dx.doi.org/10.1063/1.4973395>]

### INTRODUCTION

Co-based rare earth permanent magnetic compounds with high coercivity, high Curie temperature and narrow size distribution have drawn much attention because these can be used for obtaining high performance nanocomposite magnets and soft/hard exchange coupled magnets.<sup>1-4</sup> The Co-based rare earth nanoflakes are a promising material to prepare high-performance nanostructured permanent magnets.<sup>5,6</sup> Many Co-based rare earth permanent magnets have been obtained by the SABM method. Nevertheless, most of the experiments were based on the rare earth elements of Sm or Pr,<sup>7,8</sup> which were expensive for application. If Sm or Pr can be replaced by the low cost mischmetal, the cost of Co-based rare earth permanent magnets would be greatly reduced and the application would be widely extended. Because the purification and separation of rare earth element polluted the environment, the direct use of mischmetal would also play a positive role in environment protection. Our previous work indicated that the multistep (three steps) ball milling had many advantages compared with single step SABM. For example, three steps SABM could keep more complete crystallinity (relatively less defects) during the process of milling and enhance remanence ratio and coercivity.<sup>8</sup> Therefore, the  $\text{MMCo}_5$  nanoflakes of remarkable room-temperature magnetic properties were obtained by three steps SABM in this work.

### EXPERIMENT

The  $\text{MMCo}_5$  ingots were prepared by arc-melting in argon atmosphere using pure metals Co (99.99 %) and MM (28.27 wt. % La, 50.46 wt. % Ce, 5.22 wt. % Pr, 15.66 wt. % Nd, and impurities

<sup>a</sup>Corresponding author: [shenbaogen@yeah.net](mailto:shenbaogen@yeah.net)

less than 1 wt. %) with 2 wt. % excess of MM to compensate for the evaporation losses. The atom ratio of MM and Co was 1:5. The ingots were melted five times to ensure homogeneity and then annealed at 1173 K for a week under vacuum. The ingots were manually crushed and then ground down to less than 400  $\mu\text{m}$  as the coarse powders.<sup>7</sup> We put the stainless steel balls, coarse powders (the mass of about 5 g) and surfactant into milling vial. The weight ratio of stainless steel balls to powders was 20:1. Oleylamine (80-90 %) and oleic acid (99 %) was used as surfactant (the volume ratio of Oleylamine to oleic acid was 1:1) and heptane (99 %) was used as the carrier liquid. The total amount of surfactant was 20 % to the weight of the coarse powders. To prevent oxidation, all of these operations were done in argon-filled glove box. The multistep SABM experiment was performed for three steps with a GN-2 BM equipment: 4 h with the milling energy of 150 rpm; 8 h with the milling energy of 250 rpm; 7 h with the milling energy of 350 rpm. After every stage, the  $\text{MMCo}_5$  nanoflakes/resin composite was prepared by mixing the as-milled slurry with epoxy resin (about 2 mg of  $\text{MMCo}_5$  nanoflakes mixed with at least 200 mg of epoxy resin) in argon-filled glove box. After the epoxy resin solidified, we cut strips (about 2 mm long, 1 mm wide and 0.5 mm thick) from the composite for the following analysis. The phase structure was examined by the X-ray powder diffraction (XRD) (Rigaku D/Max-2400) with  $\text{Cu K}_\alpha$  radiation at room temperature. Morphology was characterized by scanning electron microscope (SEM) (XL30S-FEG). Magnetic properties were measured by a vibrating sample magnetometer (VSM) (Lakeshore 3474-140) with a field of up to 20 kOe at room temperature.

## RESULT AND DISCUSSION

Fig. 1 shows the magnetic hysteresis loops of  $\text{MMCo}_5$  nanoflakes at different stages. At first stage, with the milling 4h with the milling energy of 150 rpm, the coercivity reached to 3.71 kOe. When the experiment continued 8 h with the milling energy of 250 rpm, the coercivity increased to the maximum value of 5.89 kOe. With the experiment continued 7 h with the milling energy of 350 rpm, the coercivity decreased to 5.36 kOe. The inset in Fig. 1 shows that with the experiment was performing, the remanence ratio  $M_r/M_s$  monotonically decreased. The presence of surfactant in three steps SABM was to impede cold welding and the agglomeration of flakes during ball milling. Surfactant could lower the energies of freshly cleaved surfaces, enabling long-range capillary forces and lowering the energy required for crack propagation. Considering these reasons, the thickness of nanoflakes performed by SABM was much smaller than that performed by ball milling without surfactant. Another advantage of the SABM was to prevent the destruction of crystalline structure, which could be important for obtaining the high coercivity. The reduction of brittleness and increment of ductility led to the decrease of grain refinement efficiency when the particle size approached into

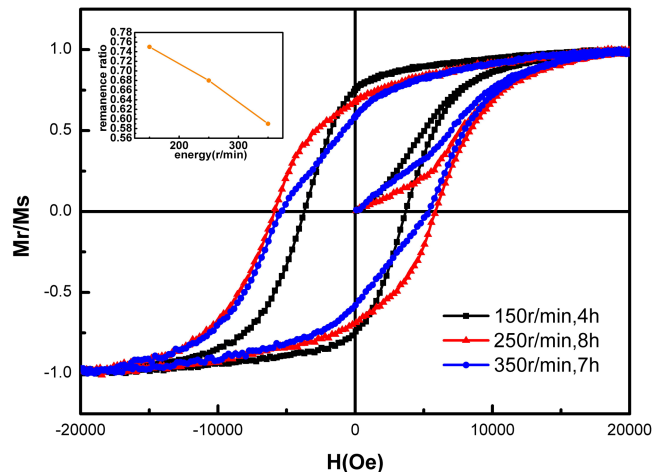


FIG. 1. The magnetic hysteresis loop and remanence ratio ( $M_r/M_s$ ) of  $\text{MMCo}_5$  nanoflakes after ball milled 4 h with the milling energy of 150 rpm; 8 h with the milling energy of 250 rpm; 7 h with the milling energy of 350 rpm; respectively.

nanocrystalline structure. The decrease of grain refinement efficiency led coercivity declined.<sup>9,10</sup> The other reason of the decline of coercivity was that increased defects in smaller particles lowered the magnetocrystalline anisotropy. It was also possible that ball milling had led to partial amorphization and smaller particles with a more amorphous structure led to reduced coercivity.<sup>10</sup> Moreover, local strains could also cause low-energy nucleation sites.<sup>11,12</sup>

Fig. 2 shows the XRD pattern of randomly oriented coarse  $\text{MMCo}_5$  powders which indicated that the main phase crystal in  $\text{MMCo}_5$  was  $\text{CaCu}_5$ -type hexagonal structure (the space group of  $\text{MMCo}_5$  is  $P6/mmm$  and the easy magnetization axis is along  $c$  axis). It can be seen that hardly any rare-earth oxides or impurity peak appeared and only the hexagonal structure was obtained, which indicated that the prepared nanoflakes had been effectively protected from oxidation during the fabrication and testing processes.

From Fig. 3c we can see that when the experiment performed 7 h with the milling energy of 350 rpm, the thickness of nanoflakes reached to the critical dimension of magnetic domain of Co-based rare earth compounds which was about  $1\ \mu\text{m}$ . The structure of magnetic domain was destructed, which might lead the decrease of coercivity. It was also proved that the size of magnetic domain of  $\text{MMCo}_5$  was about  $1\ \mu\text{m}$ . Because of the increment of small polycrystalline nanoflakes, the random orientation became inclined and the grain boundaries turned incoherence. On account of the plastic deformation, the uniaxial  $(00\ell)$  texture was decreased. The decrease of  $M_r/M_s$  also indicated that the high energy was harmful for forming textured nanoflakes. Fig. 3 shows the morphology evolution of nanoflakes with the three steps SABM. Because the  $\text{MMCo}_5$  sample was brittle and easily crushed, after ball milling 4 h with the milling energy of 150 rpm, the coarse powders were crushed down to smaller nanoflakes with the average thickness of 60 nm and in-plane size of  $1.2\ \mu\text{m}$ . With prolonging milling time up to 8 h with the milling energy of 250 rpm, the small nanoflakes become relative uniformity nanoflakes with thickness of 40 nm and a small in-plane size of  $0.9\ \mu\text{m}$ . With further milling, the thickness of nanoflakes decreased slightly to 20 nm. Compared with Fig. 1, we can see that when the thickness was between 30 nm to  $0.1\ \mu\text{m}$ , the coercivity reached to maximum while the aspect ratio increased from 20 to 60. As Fig. 4 shows, the aspect ratio was monotonically increasing, which shown the ductility of  $\text{MMCo}_5$  in nanoscale. In addition, an obvious “kebab-like” morphology formed with the submicro-flakes due to the  $c$ -axis textured and magnetostatic interaction or dipolar coupling. The inset of Fig. 3 shows the distribution of grain size performed in three steps. With the milling was going on, the thickness distribution of nanoflakes was increasingly concentrated. The thickness distribution was asymmetric normal distribution, the thicker nanoflakes was much more than the thinner. It also shows that the distribution of thin thickness nanoflakes was more and more centralized. The long time multistep (three steps) SABM will be a promising method for obtaining the centralized thickness distribution nanoflakes in practical application.

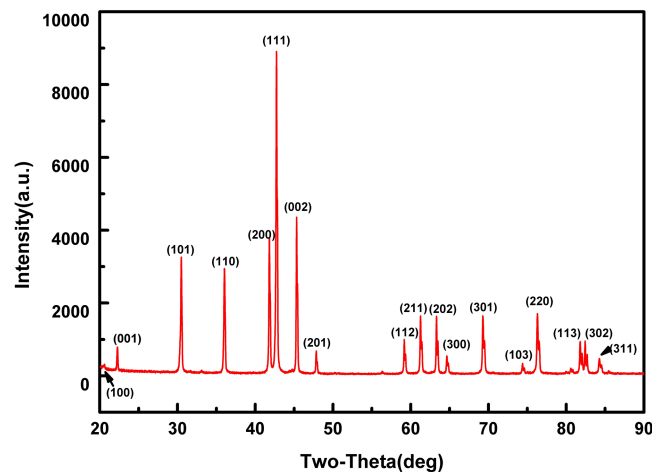


FIG. 2. The XRD patterns of randomly oriented  $\text{MMCo}_5$  coarse powders and the direction were shown near the peaks.

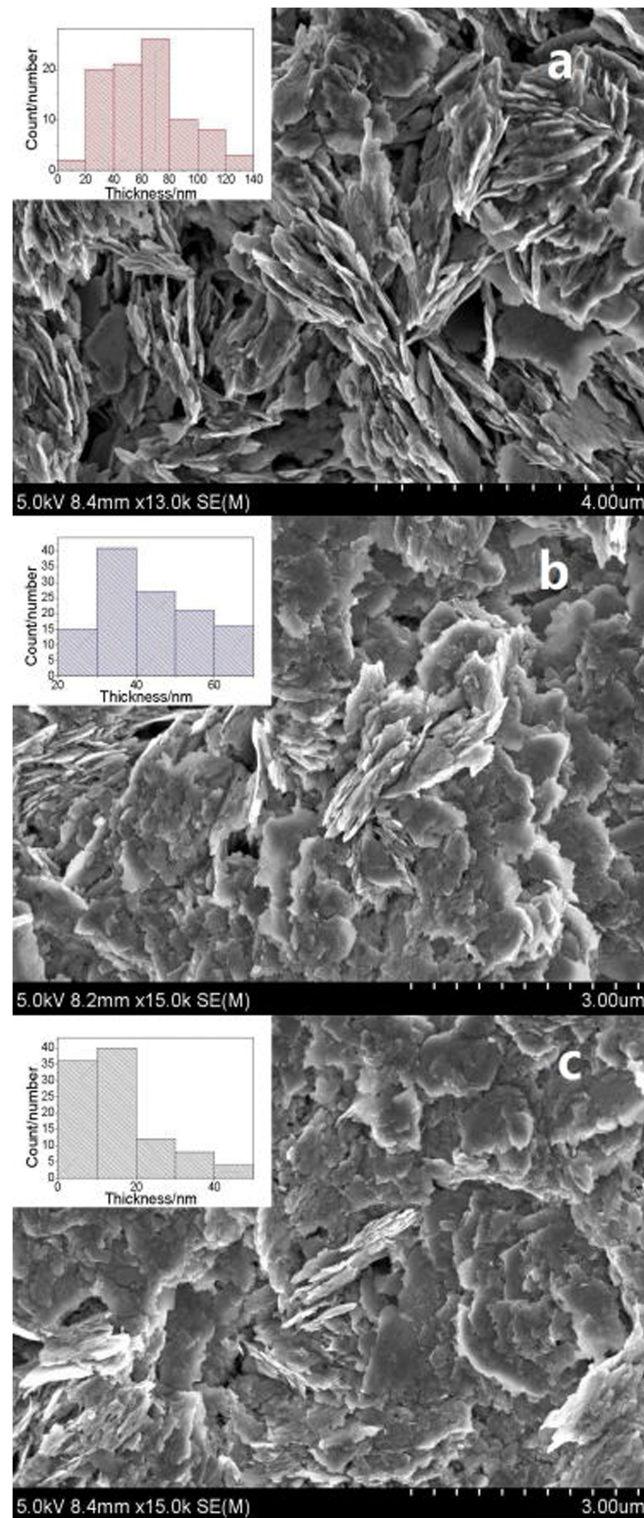


FIG. 3. The SEM images of MMCo<sub>5</sub> nanoflakes with different steps SABM energy and time. The insets show the distribution of grain size performed for three steps: a. 4 h with the milling energy of 150 rpm; b. 8 h with the milling energy of 250 rpm; c. 7 h with the milling energy of 350 rpm, respectively.

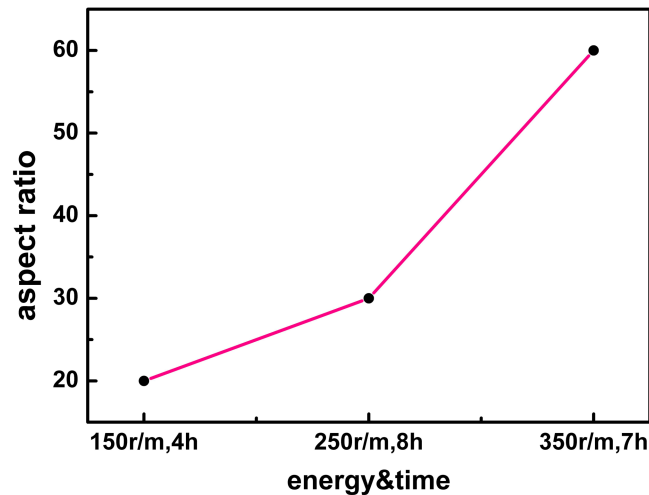


FIG. 4. The aspect ratio of  $\text{MMCo}_5$  nanoflakes obtained with different steps SABM energy and time.

## CONCLUSIONS

The low cost  $\text{MMCo}_5$  nanoflakes with large coercivity of 5.89 kOe and high remanence ratio of 0.75 were obtained by three steps SABM with the heat-treated coarse powder. The SEM results of  $\text{MMCo}_5$  nanoflakes indicated the thickness and in-plane size of ball milled samples were mainly in the range of 20-80 nm and  $1\mu\text{m}$  when SABM time reached to 19 h and with narrow size distribution. The XRD results of  $\text{MMCo}_5$  indicated the nanoflakes were  $\text{CaCu}_5$ -type hexagonal crystal structure. The  $\text{MMCo}_5$  nanoflakes with large coercivity and low cost were very promising for the future development of the anisotropy nanocomposite magnets and high performance soft/hard exchange spring magnets.

## ACKNOWLEDGMENTS

This work was supported by the National Key Research Program of China (Grant No. 2014CB643702, 2016YFB0700903), the National Natural Science Foundation of China (Grant No. 51590880) and the Knowledge Innovation Project of the Chinese Academy of Sciences (Grant No. KJZD-EW-M05).

<sup>1</sup> S. H. Sun, C. B. Murray, D. Weller, L. Folks, and A. Moser, *Science* **287**, 1989 (2000).

<sup>2</sup> H. Zeng, J. Li, J. P. Liu, Z. L. Wang, and S. Sun, *Nature* **420**, 395 (2002).

<sup>3</sup> N. G. Akdogan, G. C. Hadjipanayis, and D. J. Sellmyer, *IEEE. Trans. Magn.* **45**, 4417 (2009).

<sup>4</sup> M. Yue, Y. P. Wang, N. Poudyal, C. B. Rong, and J. P. Liu, *J. Appl. Phys.* **105**, 07A708 (2009).

<sup>5</sup> S. J. Knutson, Y. Shen, J. C. Horwath, P. Barnes, and C. H. Chen, *J. Appl. Phys.* **109**, 07A762 (2011).

<sup>6</sup> S. K. Pal, L. Schultz, and O. Gutfleisch, *J. Appl. Phys.* **113**, 013913 (2013).

<sup>7</sup> W. L. Zuo, R. M. Liu, X. Q. Zheng, R. R. Wu, F. X. Hu, J. R. Sun, and B. G. Shen, *J. Appl. Phys.* **115**, 17A728 (2014).

<sup>8</sup> W. L. Zuo, X. Zhao, J. F. Xiong, M. Zhang, T. Y. Zhao, F. X. Hu, J. R. Sun, and B. G. Shen, *Sci. Rep.* **5**, 13117 (2015).

<sup>9</sup> N. Poudyal, C. B. Rong, and J. P. Liu, *J. Appl. Phys.* **107**, 09A703 (2010).

<sup>10</sup> Y. P. Wang, Y. Li, C. B. Rong, and J. P. Liu, *Nanotechnology* **18**, 465701 (2007).

<sup>11</sup> Y. Shimada and H. Kojima, *J. Appl. Phys.* **44**, 5125 (1973).

<sup>12</sup> K. M. Chowdary, A. K. Giri, K. Pellerin, S. A. Majetich, and J. H. J. Scott, *J. Appl. Phys.* **85**, 4331 (1999).